Faunal composition and paleoenvironmental reconstruction of a Middle-Late Triassic boundary assemblage in the Pyrenean basin (Catalonia, NE Spain)

Ruben Garcia-Artigas[1,2], Ramon Mercedes-Martín[3], Joan Cartanyà[4,5], Arnau Bolet[4,6], Marc Riccetto[4] and Josep Fortuny[4]*

[1]Water Research Institute (IdRA), University of Barcelona, 08028 Barcelona, Spain. <r.garcia@ub.edu>

[2]Mineralogy, Petrology and Applied Geology Department, Faculty of Earth Sciences, University of Barcelona, 08028 Barcelona, Spain

[3]Departament de Geologia. Unitat d'Estratigrafia. Universitat Autònoma de Barcelona. Cerdanyola del Vallès E-08193, Barcelona, Spain. < info@ramonmercedes.com >

[4]Institut Català de Paleontologia, Universitat Autònoma de Barcelona. Edifici ICTA-ICP, c/Columnes s/n, Campus de la UAB, 08193, Cerdanyola del Vallès Barcelona, Spain. <joan.cartanya@icp.cat>, <arnau.bolet@icp.cat>, <m.riccetto.marti@gmail.com>, <josep.fortuny@icp.cat>

[5]Centre d'Història Natural de la Conca de Barberà C/ Pedrera, 2 – 43400 Montblanc,Tarragona, Spain

[6]School of Earth Sciences, University of Bristol, Wills Memorial Building, Queens Road, Bristol BS8 1RJ, United Kingdom

* corresponding author.

Running Header: A Triassic faunal assemblage from the Pyrenees

Abstract.—The Ladinian-Carnian transition in the Tethys domain was accompanied by an important environmental change representing a milestone in the climate evolution of the Triassic. However, estimations on paleodiversity composition and paleoenvironmental conditions across this interval are scarce in marine settings due to the lack of fossil-bearing successions. In this work, a refined paleontological and sedimentological study has allowed to better characterize a well-preserved marine ?Ladinian-Carnian carbonate succession in the South Central Pyrenees (Odèn site, Catalonia, NE Spain). Vertebrate faunas include numerous actinopterygian specimens, forming an assemblage composed of at least four taxa: *Peltopleurus* cf. *P. nuptialis*, *Saurichthys* sp., *Colobodus giganteus*, and an indeterminate halecomorph. Specimens belonging to the genus *Peltopleurus* are dominant whereas the long-snouted *Saurichthys*, the halecomorph and the large-bodied *Colobodus giganteus* are less abundant. Tetrapod remains are scarcely present and assigned to sauropterygians. Invertebrate faunas include bivalves (*Pseudocorbula gregaria*) and brachiopods (*Lingula* sp.). The fossil assemblage was recovered from organic-rich laminated silty mudstone layers. Sedimentological and textural analyses suggest that fossil biotas were deposited below the fair-weather wave base in shallow subtidal coastal settings. These environments were sporadically sourced by silt/ clay. The age of the Odèn site based on the recovered fauna is assigned to the ?late Ladinian – middle Carnian (Middle-Late Triassic), which is in agreement with previously published ages based on palynomorph data.

The refined integration of paleontological, sedimentological and biostratigraphic data from the Odèn site and other vertebrate-bearing localities in the Tethys domain can help better constraint the paleoenvironmental conditions and paleogeographical configuration impacting ecosystem diversity during the late Ladinian – Carnian interval.

Introduction

The Upper Muschelkalk deposits of NE Iberian Peninsula have been historically and largely studied. Paleontological, sedimentological, and chronostratigraphic research conducted, particularly conducted in the Catalan Basin, have been crucial to understand the evolution of the basin and its ecosystems during this time range (e.g. Verneuil, 1854; Wurm, 1913; Schmidt, 1935; Virgili, 1958; Hemleben and Freels, 1977; Via-Boada et al., 1977; Calvet et al., 1987, 1990, 2004; Calvet and Tucker, 1988; Calvet and Marzo, 1994; Fortuny et al., 2011; Mercedes-Martín et al., 2013, 2014a,b; Escudero-Mozo et al., 2015; López-Gómez et al., 2019; García-Ávila et al., 2020, and references therein).

Some of the most relevant Upper Muschelkalk fossils have been recovered in the classical localities of Mont-ral and Alcover (Catalan Coastal Ranges) (e.g. Via-Boada, 1977; Beltan, 1972, 1975, Cartanyà, 1999; Cartanyà et al., 2015). More recently discovered fossil-bearing sites in adjacent areas such as Mora d'Ebre - Camposines have fueled a renewed interest in the paleontological study of their macrofaunal and ichnofossil assemblages (Fortuny et al., 2011; Cartanyà et al., 2019; Mercedes-Martín and Buatois, 2021) (Fig. 1). The Upper Muschelkalk deposits are represented by extensive marine carbonate units of Ladinian (Middle Triassic), and potentially earliest Carnian age based on recent palynological studies (García-Ávila et al., 2020). Faunas recovered at the Mont-ral-Alcover and Mora d'Ebre-Camposines outcrops have been referred to the late Ladinian (Middle Triassic) by Cartanyà et al. (2019).

In the present work, a detailed analysis of coeval Middle Triassic carbonate successions has been performed in the nearby Pyrenean basin (NE Iberian Peninsula)

(Fig. 1). The corresponding sites have been inadequately studied compared with their equivalent counterparts in the Catalan Coastal Ranges (Lehman, 1964; Fréchengues et al., 1990; Fréchengues and Peybernès, 1991a, b; Calvet et al., 1993, 2004; Cartanyà et al., 2011, 2015; Fortuny et al., 2011).

In the Pyrenean basin, fossil fishes are poorly known from only two localities (Fig. 1): 1) Vilanova de la Sal, with reports of an actinopterygian fauna not described in detail (Fortuny et al., 2011), and 2) Odèn, with abundant actinopterygian remains. The Odèn locality was firstly reported by Lehman (1964) who described postcranial remains assigned to *Acidorhynchus*, a genus currently considered a subjective junior synonym of *Saurichthys* (Wu et al., 2011). Later, additional specimens referred to *Saurichtys*, as well as to Peltopleuridae, Halecomorpha and to the large-bodied *Colobodus* were reported from this site (Cartanyà et al., 2011, 2015; Fortuny et al., 2011).

The purpose of this work is twofold: 1) to update and summarize the composition of the diverse faunal assemblage from the Ladinian- Carnian transition at the Odèn locality to date, including the description of the most abundant actinopterygian taxon; and 2) discuss the paleontological, chronostratigraphical, and paleoenvironmental implications of this faunal assemblage in the context of adjoining Middle Triassic basins of the Tethys region.

Geological setting

On the Iberian Peninsula, the Triassic stratigraphic record can be subdivided into three parts, from the base to the top: Buntsandstein facies (continental clastic sediments forming red beds), Muschelkalk facies (marine carbonates, evaporites and red beds), and Keuper facies (tidal and sabkha deposits) (Virgili et al., 1983; Salvany and Ortí,

1989; Calvet et al., 1990). From a tectonostratigraphic point of view, the evolution of the Iberian Peninsula during the upper Permian and Mesozoic can be divided into three rifts and their corresponding post-rift stages, which controlled the sedimentation styles. The rift cycle corresponding to the late Permian - Triassic mainly affected the eastern part of the Iberian plate, giving rise to basins that were filled with sediments attributed to the Germanic facies during the late Permian and Triassic (Salas and Casas, 1993; Ramos et al., 1996; Salas et al., 2001).

In the South Pyrenean sector (Les Nogueres-Cadí), the Muschelkalk facies lies on top of the Buntsandstein facies (Anisian), which is composed by sandstones, conglomerates, and clay deposits. The Upper Muschelkalk of the South Pyrenean sector is represented by several limestone-marl-dolostone units of Anisian to Ladinian age (Fréchengues et al., 1990, 1991, 1992; Fréchengues and Peybernès, 1991a, b; Calvet et al., 1993). From base to top, the Upper Muschelkalk is an assemblage of marly dolostones, grey limestones, and limestones with laminated dolostones (Fig. 1) deposited in laterally restricted carbonate ramp intertidal to subtidal environments potentially equivalent to those in the Catalan Coastal Ranges. The total thickness of the Upper Muschelkalk facies in the South Pyrenean region ranges between 37 and 108 meters according to Calvet et al. (1993). In this sub-basin, the Muschelkalk facies can be subdivided into three lithological units from bottom to top: Marly Dolomites Unit (2 to 8 meters thick), Grey Limestone Unit (20 to 70 meters thick) and Laminated Limestone and/or Dolomites Unit (15 to 30 meters thick) (Calvet et al., 2004) (see Fig. 1).

The studied outcrops at the Odèn locality can be broadly assigned to the Laminated Limestone and/or Dolomites Unit of Calvet et al. (1993), who proposed a late Ladinian – middle Carnian age for these units based on palynological data.

Material and Methods

A 28.5-meter long composite sedimentary section was logged at the Odèn locality. The base of the section can be found in the kilometric point 29 of L-401 road, between the villages of Coll de Nargó and Odèn (Figs. 1 and 2). Thirteen rock samples were collected for thin-section analyses. Sedimentary textural descriptions were carried out with a Nikon Eclipse 8400 optical microscope, and photomicrographs were taken with an attached Nikon Microphot FX camera. The material studied here was collected starting in 2009 and were followed by some additional paleontological excavations in 2010, 2016, and 2020, yielding a total of 450 specimens (see Results section). All field campaigns were performed under legal permits issued by Departament de Cultura of the Generalitat de Catalunya (Catalan local government). Nine actinopterygian specimens (genus *Peltopleurus*) are described in detail for the first time in this work (IPS85811, IPS86048, IPS106902, IPS106957, IPS106977, IPS122561, IPS107023, IPS85919 and IPS106909). All actinopterygian specimens underwent chemical and mechanical preparation. The chemical preparation included swabbing the pieces with formic acid (5%) and mechanically removing the matrix surrounding or covering the skeleton using a thin needle under a stereomicroscope. The specimens were imaged by using a binocular Leica MZ 16A and line drawings were made with Corel Draw© software.

Repositories and institutional abbreviations.— All specimens examined in this study are deposited in the: Institut Català de Paleontologia Miquel Crusafont (Sabadell, Spain) and are labelled using the acronym IPS.

Systematic Paleontology

Subclass Actinopterygii Cope, 1887

Order Peltopleuriformes Gardiner, 1967

Family Peltopleuridae Brough, 1939

Genus *Peltopleurus* Kner, 1866

Figures 3-9

Peltopleurus cf. *P. nuptialis*

Type species.— *Peltopleurus splendens* Kner, 1866. Its type locality is Raibl, Carinthia which is in a Julian marine limestone in Italy

Occurrence.— Lower levels of organic-rich laminated mudstones from the facies association 1 (organic-rich laminated silty mudstone). Laminated Limestone and/or Dolomites Unit of Calvet et al. (1993).

Description.— General morphology. *Peltopleurus* cf. *P. nuptialis* has a fusiform body with a forked caudal fin and presents general features that all the species of *Peltopleurus* share (see below). This taxon has two distinct morphotypes (herein named as morphotype A and B, respectively) with differences in the pectoral, pelvic, anal, and dorsal fins and in the rostral bone. Its maximum standard length is 25 mm, with a total length of 29 mm and a head length constituting around 34% of the standard length.

Snout.— The rostral bone has a rounded convex shape with differences representing two morphotypes. In morphotype A, this bone presents a smoothed surface, whereas morphotype B specimens show at least two prominent conical tubercles with a maximum height of 0.3 mm (Figs. 3.1 – 3.2 and 4). The nasal bone has a convex shape with a small notch for the anterior nostril on its anterior margin (Figs. 3.3 and 4). It contacts the rostral bone. These two elements are in contact with the frontal, the premaxilla, and possibly with the antorbital. However, this character cannot be discern with confidence in any recovered specimen. The premaxilla is rectangular, bearing two big conical teeth on its oral margin (Figs. 3.2 and 4).

Skull roof.— The frontal bone is broad and expanded in its posterior part and narrower anteriorly. The surface of the frontal bone has at least 16 small conical tubercles randomly arranged (Figs. 4 and 5). The parietal bone has a smooth surface and its contact with the frontal bone is straight (Figs. 4 and 5). There is a ridge parallel to the orbital margin of the frontal and parietal bones identified as the supraorbital sensory canal. The subrectangular dermopterotic (Fig. 3.1) is placed in contact to the frontal, parietal, the extrascapular and the suborbital (Figs. 3 and 4). The extrascapular and the post-temporal are not well preserved due to the disarticulation of the skulls.

Circumorbital series.— There are two infraorbitals (Figs. 3 and 4). The first infraorbital is in contact with the antorbital, the premaxilla, and the distal part of the maxilla whereas the second infraorbital is the largest one, being in contact with the rest of the maxilla and half of the preoperculum. The dermosphenotic is similar in size to the first infraorbital, being in contact with the second infraorbital, the rest of the preoperculum and the suborbital, the frontal and one supraorbital. No dermohyal is observed due to preservational reasons. The supraorbitals are not well preserved in any

recovered specimens due to the state of preservation. However, in one specimen (Fig. 3.1) it is possible to discern a potential supraorbital.

Cheek bones.— The suborbital is large and triangular with rounded edges and contacts the preoperculum, the operculum, the dermopterotic and the skull roof bones (Figs. 3 and 4).

The preoperculum is trapezoidal with its upper and lower margins narrower than the central portion. Its anterior margin is in contact with the infraorbitals 2 and 3. Its posterior margin is in contact mainly with the operculum but also with the subopercular. On its lower margin, the preoperculum is in contact with the maxilla and its upper margin is in contact with the suborbital (Figs. 3 and 4). The posterior margin shows a ridge parallel to the margin identified as the preoperculum sensory canal.

The maxilla shows a thin anterior part and a broad rounded posterior one. The oral margin bears at least 14 sharp conical teeth of different heights (Figs. 3 and 4). The anterior margin is in contact with the premaxilla and the posterior part of the maxilla is in contact with the preoperculum and the cleithrum. The palatal bones bear several rows of flattened oval teeth hinting at a semi-durophagous diet (Fig. 7.3).

Opercular series.— The operculum and the subopercular bones are D-shaped. The operculum is large and in contact with the preoperculum and the suborbital on its anterior margin and the cleithrum on its posterior margin (Fig. 3 and 4). The subopercular has a straight contact with the operculum. This subopercular is significantly smaller and in contact with the maxilla on its anterior margin.

Lower Jaw.— The dentary bone shows a narrow anterior portion and an expanded posterior end, with at least one small notch on its middle part (Figs. 3.3 and 4). The oral margin bears at least 16 sharp conical teeth of different height, slightly larger than those of the maxilla.

Girdles and paired fins.— The shoulder girdle is composed by a robust cleithrum. It is sickle-shaped, with an irregular surface, and a shorter supracleithrum (Figs. 3 and 4). The cleithrum is in contact with the posterior margin of the operculum and subоperculum (Figs. 3.1 and 4). The branchiostegal rays are not preserved in any specimen due to the fragility of these bones and the poor preservation of this area of the skull.

The pectoral fin is long and made of at least seven distally segmented rays. On the specimens referred to morphotype B these rays consist of a long proximal segment and at least seven shorter segments (Figs 6 and 7.1). The unsegmented anterior ray bears six sharp hooks on its anterior margin, followed by the first segmented ray showing at least 7 hooks along its anterior margin. The rest of these segmented rays show a single hook on the distal margin. Specimens referred to morphotype A present a shorter fin, with the same structure but without hooks. The pelvic fin is smaller than the pectoral fin, composed by at least 8 rays and showing the same structure of rays and hooks as on the pectoral fin (Fig. 6).

Median fins.— The dorsal fin is made of long lepidotrichia, composed of at least 10 distally segmented rays and four basal fulcra (Fig. 7.2). On morphotype B, the segments from the anterior ray show a sharp hook on each fragment whereas in morphotype A these rays are shorter and without any hook.

The anal fin shows two different patterns. In morphotype B, this anal fin is made of at least eight rays with a minimum of five segments bearing hooks. Above these rays there are an indeterminate number of very thin rays ending in small sharp hooks. This fin is partially covered by a triangular scute (Fig. 8). In morphotype A, this anal fin is formed of at least 14 rays with a minimum of five segments missing the hooks and the scute.

The caudal fin is hemiheterocercal with a forked profile and composed of 24 principal rays made up of a minimum of 8 segments (Figs. 6 and 9). There are four basal fulcra on each lobe and four or five epaxial rays on the upper lobe. However, the state of preservation precludes to distinguish more details of the caudal fin as the fringing fulcra and procurrent rays.

Squamation.— The scale covering is made up of 35 or 36 vertical smooth scales rows along the lateral line of the body (Figs. 6 and 9). The lateral-line scales are sigmoidal and increase in depth on the anterior part of the body and decrease in size to the posterior part. There are two rows of rectangular scales on the dorsal margin above the lateral-line scales and one row on the ventral margin below the lateral line scales (Fig. 9). All the scales have a small spine on the posterior margin (Fig. 9). The caudal region is made up of five triangular scale rows.

Material.— IPS106977, anterior part of the body. IPS106957, a complete body missing the anterior part of the skull. IPS107023, a poorly preserved body including the skull. IPS86048, a nearly complete body with its disarticulated skull and all the fins. IPS85811, a partially disarticulated body showing some cranial features. IPS106902, a partially disarticulated body with a good preservation of some fin characters. IPS122561, anterior part of the body preserving most of cranial bones. IPS85919, a partially disarticulated body showing some features of the fins. IPS106909, a poorly preserved body showing some cranial features.

Remarks.— The small size of the body, the presence of a big operculum, a tall preoperculum and a hemiheterocercal caudal fin are diagnostic characters of Peltopleuriformes (Gardiner, 1967). Recently, Xu and Ma (2016) defined

Peltopleuriformes *sensu stricto* including only Peltopleuridae and Thoracopteridae. The monophyly of these clades, based on Xu and Ma (2016) analyses, is well supported by five synapomorphies: supraorbital sensory canal ending in the frontal; absence of a preoperculum/dermopterotic contact; presence of a postpiracle; presence of dense brush-like rays articulating proximally with several stout segments in the male anal fin; and presence of enlarged lateral scutes associated with the anal fins. All these characters are identified on the Odèn specimens, except the presence of postpiracle, not observed probably by preservation reasons.

Regarding Peltopleuridae, the original diagnosis of this group provided by Brough (1939) include as diagnostic characters the small size of the body, large orbits, fins of small to moderate size, hemiheterocercal forked tail, deep flank scales, frontals large and elongated, rectangular parietals, long and narrow supratemporals, wide preoperculum attached to the maxilla, large operculum, small suboperculum, and few branchiostegal rays. All these characters are identified on the Odèn specimens with the exception of the branchiostegal rays, which are not preserved. Brough (1939) marked as a diagnostic character a weak dentition with minute teeth on the maxilla, or no teeth at all. However, Lombardo (1999) noted that this character is not really diagnostic for Peltopleuridae due to the strong dentition present in *Peltopleurus notocephalus* and *Peltopleurus nuptialis* (Bürgin, 1992; Lombardo, 1999). For this reason, Lombardo (1999) questioned the diagnosis of Brough (1939), although she did not present an emended diagnosis of this family.

Peltopleurus is a genus included within the clade Peltopleuridae, including 12 species, from Middle to Upper Triassic. This genus have been recovered from Austria, Italy, Spain, Switzerland and South China (Kner, 1866; Brought, 1939; Beltan, 1972, 1975; Bürgin, 1992; Lombardo, 1999; Cartanyà, 1999; Xu and Ma, 2016; Xu et al.,

2018). It was erected on the basis of a unique combination of characters (Kner, 1866): i) a small fish with a fusiform body, in agreement with the Odèn specimens with an average ratio of total length - maximum body depth of 3.89; ii) a flank with a longitudinal row of tall scales; the specimens from Odèn show that longitudinal row of deep scales; iii) a vertical preoperculum and a maxilla with a narrow anterior region and an expanded postorbital; this vertical preoperculum and this narrow morphology on its anterior part and expanded on its posterior part maxilla are also present on the specimens from Odèn; iv) the presence of a wide and semicircular opercular region; the opercular region in the specimens from Odèn is broad and D-shaped, matching with the description for this genus; v) caudal fin externally symmetrical, as present on the Odèn specimens. vi) a short axial body lobe with at least six epaxial rays. On the specimens reported here, the axial body is short and there are at least four or five epaxial rays. All aforementioned characters support the attribution of reported specimens from the Odèn site to the genus *Peltopleurus.*

Differences on the pectoral, pelvic, anal and dorsal fins as well on the rostral bone reveals the presence of dimorphism in the Odèn taxon. Morphotype A has a pectoral fin made of at least seven rays distally segmented, a pelvic fin with at least eight rays distally segmented, an anal fin composed by at least 14 rays distally segmented, a dorsal fin composed by at least 10 rays distally segmented, and the rostral bone being rounded and smoothed. Morphotype B has a pectoral fin made of at least seven rays distally segmented and much longer than those of morphotype A; moreover, morphotype B presents the following characters: the anterior unsegmented ray bears on its anterior margin six sharp hooks, followed by the first segmented ray bearing at least seven hooks along its anterior margin. The rest of these segmented rays show: a single hook on its distal margin; a pelvic fin with at least eight rays distally segmented with the

same hook structure as the pectoral fin and an anal fin made of at least eight rays composed by a minimum of five segments bearing hooks. Above these rays there is an indeterminate number of very thin rays ending in small sharp hooks. This fin is partially covered by a triangular scute. The dorsal fin is composed of at least 10 rays distally segmented, the segments from the anterior ray show a sharp hook on each fragment and the rostral bone is rounded and it has a prominent tubercle.

The presence of two morphotypes with differences mainly related to fin morphology is know from *Peltopleurus* species such as *P. nuptialis*, where what would correspond to our morphotype A is assumed to be a female and morphotype B would represent the male as shown by the presence of hook structures as discussed in Lombardo (1999).

The specimens herein described present similarities with the specimens referred by Lombardo (1999) to *Peltopleurus nuptialis*, erected on basis to the following combination of features. Small species of *Peltopleurus*, up to 25 mm standard length with 32 vertical scale rows. Our specimens share this standard length but with 35 or 36 scale rows. Two scales rows dorsal to the deepened flank scales and one ventral. The specimens recovered in the Pyrenees show the same squamation pattern. Posterior margin of all scales with one to three small spines. The specimens herein described show only one spine on the posterior margin of all scales. All fins, except for the caudal one, have anterior margins bearing a series of hook-like structures. These hook structures are identified in our specimens on all the fins except the caudal one. There is distinct sexual dimorphism.

Despite the similarities between *P. nuptialis* and the specimens herein described shown on the diagnosis, some differences are worth highlighting. The pectoral fin in the Odèn specimens seems to be significantly longer than the pectoral fin on *P. nuptialis*. The frontal bones in the specimens from Odèn have at least 16 small conical tubercles

randomly arranged, feature not identified on *P. nuptialis*. The cleithrum on the Odèn specimens seems to be longer than that described in *P. nuptialis*. Considering the state of preservation of the specimens described herein, we decided to keep a conservative taxonomic assignation and, although subtle differences with *P. nuptialis* exist, we prefer to assign these specimens to *Peltopleurus* cf. *P. nuptialis*. Some characters are not well preserved in the Odèn specimens and additional data are required to assess with confidence the taxonomical assignment of this material.

Results

Summary of macrofaunal assemblages at Odèn locality.— The first fossil recovered from Odèn consisted of postcranial remains referred to *Saurichthys* sp. by Lehman (1964). Calzada and Magrans (1997) reported a lingulate brachiopod. A second specimen of *Saurichthys*, a lower jaw, was described by Cartanyà et al. (2011). Finally, a skull of the large-bodied colobodontid *Colobodus giganteus* was also recovered and described in detail by Cartanyà et al. (2015).

More than 90% of the body fossils recovered during last field campaigns (see Methods for further details) belong to vertebrates and only about 10 invertebrate specimens are referred to the bivalve *Pseudocorbula gregaria* (Fig. 10.1); among the vertebrate fossils, almost 60% belong to *Peltopleurus*, around 15% belong to indeterminate actinopterygians (Fig. 10.3), and 20 specimens are referred to *Saurichthys* (representing almost 10% of the total samples, mostly representing lower jaws and, to a lesser extent, cranial bones). Around 20 specimens (representing almost 10% of the total samples) have been tentatively referred to an undetermined halecomorph actinopterygian; furthermore, few additional poorly preserved colobodontid remains have been also

discovered. Furthermore, there are 10 ribs and teeth tentatively referred to sauropterygian reptiles (Fig. 10.2).

Facies description .—Three facies associations were identified based on depositional texture, skeletal and non-skeletal components, sedimentary features, and lateral relationships (Figs. 11, 12 and 13). The recognition of facies heterogeneities across the studied area enabled the identification of the sedimentary environments.

Facies association 1: Organic-rich laminated silty mudstone.—This facies consists of an up to 11.5 m thick, laterally restricted alternation of 30- to 80- cm-thick dark grey to pale brown, fetid and organic-rich finely laminated silty mudstones with up to 2-m-thick massive and organic-rich mudstone (Fig. 11.1 - 11.2). Most massive layers show planar to slightly undulated bottom contacts. Rare intervals exhibit channel-fill structures with fining-upward cross-bedded bundles over erosional, sharp bases (Fig. 11.1). In places, up-to-10-cm-thick intraclastic packstone, or up to 40 cm-thick brown marly clay intervals are interbedded within the finely laminated units. Some metric-scale slumped and fractured beds are recognized in the massive intervals. The major allochems are carbonaceous intraclasts (up to 1 mm wide), plant remains (up to 1 cm wide), fish coprolites (up to 1 cm wide), fish scales, peloids, thin-shelled bivalve intraclasts, and unidentified microfossil remains (Fig. 11.3 - 11.4). Trace fossils are absent, but the organic-rich mudstone component of this facies yielded a fish assemblage comprising at least four taxa (see below), scarce tetrapod remains assigned to marine reptiles (sauropterygians), bivalves (*Pseudocorbula gregaria*), and brachiopods (*Lingula* sp.). Most actinopterygians referred to *Peltopleurus* were found in the laminated lower levels, whereas the halecomorph specimens were recovered from

400 the upper horizons. In contrast, *Saurichthys* specimens were regularly found throughout
401 the entire facies (Fig. 14).
402 The thin lamination, absence of bioturbation, good preservation of the
403 actinopterygian remains (retaining organic matter and remaining articulated), and
404 scarcity of *in-situ* benthonic fossils suggest anoxic/dysoxic conditions.
405 The depositional texture and sedimentary features of facies association 1 suggest
406 deposition below the fair-weather wave base under relatively low-energy conditions in
407 shallow subtidal marine environments episodically sourced by silt and clay. However,
408 the presence of *Pseudocorbula gregaria* might indicate the proliferation of such
409 bivalves during periods of limited terrigenous input (García-Gil, 1991). The thinly
410 bedded organic-rich and undisturbed mudstone laminae suggest both low-energy
411 environments and recurrent oxygen deficiency at the sea bottom leading to anoxic to
412 suboxic conditions that probably enhanced fossil fauna preservation. The diversity of
413 vertebrate fauna encountered in this facies association suggests enough water depth to
414 support nektonic lifestyles. Channel-fill structures over erosional bases suggest the
415 circulation of sporadic sea-bottom currents (Fig. 14).
416
417 Facies association 2: Laminated silty mudstone to wackestone.—Facies association
418 2 is made up of 8 m thick, laterally continuous (up to 400 m wide) thinly bedded
419 alternation of centimeter-thick silty pale grey mudstone to wackestone with millimeter-
420 thick dark brown-grey silt to clay laminae (Fig. 12). The tops of the limestone-rich
421 intervals exhibit persistent wave ripple structures with straight, symmetrical, and
422 parallel crests (Fig. 12.1). Ripple marks range between 0.5 to 1 cm in length, and
423 normally are 0.5 cm in height. Inter-ripple depressions are silt-rich and in many cases
424 dewatering structures occur (Fig. 12.2 – 12.4). Flame structures tend to leave open

porosity conduits at 45º to 80º from ripple planes, which are partially filled by silt or cement (Fig. 12.3 – 12.4). Convolute lamination is observed as slightly folded and unbroken layers (up to 15cm in height) with arcuate crests (Fig 12.2) laterally extending over 20 to 100 cm in outcrop. The siliciclastic proportion of this facies is slightly increased towards the eastern section of the outcrops where dewatering structures are growingly less evident.

The depositional texture and lateral stratigraphic distribution of this unit suggest sedimentation in shallow subtidal to intertidal mud flats with variable contributions of silt and clay in a coastal environment. The low frequency of the ripple bedforms and their elongated, parallel crests suggest low to moderate hydraulic conditions in wave-influenced settings.

Facies association 3: Slumped and collapsed breccia deposits.—This facies association consists of between 2-to-8-m-thick laterally restricted unit of slumped and contorted beds dominated by poorly sorted, mainly clast-supported breccia and blocks (5 to 60 cm in diameter) (Fig. 13). This unit is pinching out towards the eastern part of the outcrop. Most of the blocks are made up of sub-consolidated silty mudstone to wackestone (Facies Association 2) and, to a lesser extent, of reworked organic-rich laminated silty mudstone (Facies Association 1) (Fig. 13.1 – 13.2). The former is more abundant towards the western area of the outcrop.

According to the depositional texture and the stratigraphic relationships, this facies is interpreted as a restricted gravitational collapse formed by remobilization of the shallower facies association 2 on top of the deeper facies association 1. The lateral thickness variations of facies association 3 suggest rising water depths westwards with an increase in deposition of reworked and contorted laminated silty mudstones towards

such direction. Gravity-flow deposition could be triggered by storm events or syntectonic activity as identified in adjacent coeval Middle Triassic areas of the Catalan Basin (Mercedes-Martín and Buatois, 2021).

Discussion

Faunal assemblage. —The macrofaunal assemblage recovered at the Odèn site includes two invertebrate taxa: a lingulate brachiopod and the bivalve *Pseudocorbula gregaria*. Aside from being less diverse, invertebrates are in appearance volumetrically less abundant in comparison with the fish assemblage present. In this assemblage, the genus *Peltopleurus* is highly dominant. Less common taxa are represented by the colobodontid *Colobodus giganteus*, the long-snouted *Saurichthys*, and an indeterminate halecomorph. Specimens of *Saurichthys* can only be identified at the genus level, in agreement with previous reports by Lehman (1964), Cartanyà et al. (2011) and Fortuny et al. (2011).

The Odèn fish assemblage is comparable to that found at the coeval locality of Vilanova de la Sal (Fig. 1). This site is particularly known for the presence of a semi-articulated specimen of a pachypleurosaur sauropterygian (Fortuny et al., 2011), as well as some fragmentary actinopterygian fossils including *Peltopleurus* and *Saurichthys* that have never been described in detail. Furthermore, the site yielded specimens tentatively attributed to the genus *Eosemionotus* (Fortuny et al., 2011), a taxon unknown so far from the Odèn site. *Colobodus*, halecomorphs, and invertebrates are apparently absent in the Vilanova de la Sal outcrops, although the site has been less extensively sampled. Additional taxonomic and sedimentological work, as well as a more extensive sampling at Vilanova de la Sal site and coeval locations in the neighboring sub-basins are

475 required to better reconstruct the Pyrenean paleoecosystems during the Middle-Late
476 Triassic transition.

477 Although the fossil-bearing sites at Mora d'Ebre-Camposines and Mont-ral-
478 Alcover are roughly coeval with the Pyrenean Odèn site (as all of them are situated in
479 Upper Muschelkalk facies), they are characterized by different faunal assemblages. For
480 example, the Mora d'Ebre-Camposines site displays an important assemblage of
481 invertebrates, particularly ammonoids (including *Protachyceras hispanicum*,
482 *Protachyceras vilanovae*, *Anolcites sp.* and *Iberites pradoi*), thylacocephalans, and
483 bivalves (dominated by *Daonella*) (Cartanyà et al., 2019), none of which have been
484 recovered at Odèn. This is consistent with the particular geological context of the Odèn
485 site, located adjacent to more restricted coastal mud flats compared to Mora d'Ebre-
486 Camposines that were likely situated in more open marine settings. In addition, the
487 Ladinian vertebrate fauna in Mora d'Ebre-Camposines is dominated by the perleidid
488 actinopterygian *Moradebrichtys vilasecae*, although *Saurichtys* is also present. Overall,
489 the faunas and environments at Mora d'Ebre-Camposines and Odèn are clearly different
490 and might correspond to slightly different ages with the Odèn outcrops potentially
491 slightly younger.

492 On the other hand, Mont-ral – Alcover record a greater number of invertebrate
493 and vertebrate specimens. Nektonic and planktonic organisms are dominated by
494 actinopterygians, sauropterygian reptiles, cephalopods, and swimming decapods, among
495 others. Benthic forms like reptant decapods, crinoids, limulids, holothurids, and
496 brachiopods are present but not dominant (Via-Boada et al., 1977). Up to 13 families of
497 actinopterygians are recorded in the Mont-ral – Alcover outcrops. Of particular interest,
498 saurichthyids are abundant, including *Saurichthys*. However, *Peltopleurus*,
499 *Eosemionotus*, *Perleidus* and *Colobodus*, are also present (Cartanyà, 1999).

Differences in faunal diversity between the Mont-ral –Alcover and Odèn sites are striking despite the fact that some taxa (e.g. *Peltopleurus*, *Saurichthys*, *Colobodus* and marine reptiles) can be found in both assemblages. We acknowledge that taphonomic and sampling bias possibly exists, and future surveys will help to get a clearer picture of the faunal composition in these settings. Despite the Catalan Coastal Ranges sub-basin (Mont-ral –Alcover sites) and the Pyrenean sub-basin (Odèn site) recorded peritidal to subtidal marine deposition during the Middle Triassic times, more work is required to further reconstruct the paleogeography and the degree of connectivity between both sub-basins during the Ladinian-Carnian.

Chronostratigraphical implications. —The age of the Odèn fossiliferous levels is difficult to constrain, but potentially ranges from the ?late Ladinian to the early - middle Carnian. The possible oldest age (?late Ladinian) can be assumed based on the presence of the actinopterygian genus *Peltopleurus*, which is also recovered from the late Ladinian of Montral-Alcover (Cartanyà, 1999). Indeed, lateral equivalent carbonate units have a late Ladinian – early Carnian age based on palynomorph associations (see García-Ávila et al., 2020). Nonetheless, it should be noted that *Peltopleurus* is also known from even older stratigraphic intervals (Anisian and Ladinian) at Monte San Giorgio (Lombardo, 1999; Furrer et al., 2008). Thus, a greater age cannot be completely ruled out based only on the presence of the actinopterygian *Peltopleurus*.

On the other hand, the palynological assemblage identified in the Laminated Limestone and/or Dolomites Unit in Odèn has been dated to the middle Carnian (Calvet et al., 1993).

Paleonvironmental and paleogeographic implications.—The Upper Muschelkalk carbonate sedimentation in the Triassic Catalan Basin (NW Spain) probably took place in extensive fault-block marine carbonate ramp settings during periods of rapid syn-rift subsidence (Calvet and Tucker, 1988, Mercedes-Martin et al., 2013). However, the sedimentological and paleogeographical setting of the co-eval deposits in the South Pyrenean basin (NE Spain) is less well resolved (Calvet et al., 1993).

The present work refines the sedimentary and paleoenvironmental context of the Upper Muschelkalk to Keuper facies transition outcropping at Odèn (Fig. 14). The study of lateral and vertical facies relationships has permitted the recognition of two types of sedimentary environments, from laterally extensive shallow subtidal-intertidal coastal mud flats to more restricted and deeper subtidal settings. The occurrence of gravity flow deposits (facies association 2) and syn-sedimentary slumped and contorted beds in facies association 1 suggest active fault-block instability likely involved in facies differentiation. The slightly steeped paleoslope toward the west is thought to segregate the shallower coastal silty mud flat areas and the deeper subtidal and low energy settings, where abundant vertebrate faunas proliferated. Rapid lateral facies shift suggests a strong degree of basin compartmentalization in the Pyrenean sector when compared with the time-equivalent facies in settings of the Coastal Catalan Ranges (e.g., Gaia or Priorat domain, Mercedes-Martín et al., 2013). In the former settings, sedimentary architectures of kilometer scale have been recognized with more gradual facies lateral changes. Despite such differences, the tectonic compartmentalization of these marine basins is thought to have favored the preferred development of taphonomic traps in subtidal settings where enhanced faunal preservation occurred.

The predominance of silty and clay-rich carbonate facies in the Odèn outcrops contrasts with the conspicuous absence of terrigenous sediment portions in the Triassic

549 Coastal Catalan Ranges. This suggest that the region of Odèn represents land attached
550 setting where shallow subtidal- intertidal carbonate coastal deposition was influenced
551 by silt/ clay sources, while in the Coastal Catalan Ranges more open marine conditions
552 prevailed.
553

554 ## Conclusions

555

556 Recent paleontological surveys in the Upper Muschelkalk to Keuper deposits at Odèn
557 (Pyrenean basin) have provided new faunal data suggesting that this location can hold
558 the key to better clarify the poorly known local ecosystem composition and shed light
559 on the diversification among peltopleuriform actinopterygians during the Middle
560 Triassic.

561 To date, the faunal assemblage includes, at least, four actinopterygian taxa:
562 *Peltopleurus* cf. *P. nuptialis*; *Sauricthys* sp.; *Colobodus giganteus*, and an indeterminate
563 halecomorph. A few disarticulated remains document the presence of sauropterygian
564 reptiles (Fig. 14).

565 The age range of the organic-rich laminated silty mudstone fossil-bearing units is
566 considered to be ?late Ladinian – middle Carnian based on palynomorph associations
567 (Calvet et al., 1993). The depositional environments where the faunas existed suggest
568 sedimentation in shallow subtidal, low-energy coastal settings, below the fair-weather
569 wave base and sourced by sporadic silt/ clay. Deposition in organic-rich laminated silty
570 mudstone intervals might have led to preservation of the vertebrate remains under
571 anoxic conditions. The tectonically driven compartmentalization of these marine basins
572 played a key role favoring subtidal settings as taphonomic traps for enhanced faunal
573 preservation in the studied site and likely in other locations of Tethys domain. Despite

574 the fact that the Catalan Coastal Ranges sub-basin (Mont-ral –Alcover sites) and the
575 Pyrenean sub-basin (Odèn site) were dominated by peritidal to subtidal sedimentation
576 during Middle Triassic times, more work is warranted to further reconstruct the
577 paleogeography and the degree of connectivity between these sub-basins and the Tethys
578 sea during the Ladinian-Carnian interval.
579

580 ## Acknowledgements

581 Special thanks to E. Solà, A. Sagarra, A. G. Sellès, M. Petruzzelli, E. Mujal, M. Vilalta,
582 A. Lecuona, M. Fernàndez-Coll, B. Vila, À. Galobart and J. Marmi for fieldwork
583 support. J. Gallemí and S. Calzada (Barcelona, Catalonia) are acknowledged for their
584 contribution on relevant information about the site. I. Casanovas-Vilar (ICP) is
585 acknowledged for imaging support. The authors acknowledge the logistic support of the
586 Odèn town council and "Centre de Natura d'Odèn". J.F. is a member of the
587 consolidated research group (GRC) 2017 SGR 86. A.B. is supported by a Juan de la
588 Cierva Incorporación Fellowship (IJC2018-037685-I, funded by Ministerio de Ciencia e
589 Innovación of the Spanish Government). We acknowledge support from the CERCA
590 programme (ICP) from the Generalitat de Catalunya, and the projects "Vertebrats del
591 Permià i el Triàsic de Catalunya i el seu context geologic" (Ref 2010/70085), "Evolució
592 dels ecosistemes amb faunes de vertebrats del Permià i el Triàsic de Catalunya" (ref.
593 2014/100606) and "Evolució dels ecosistemes durant la transició Paleozoic–Mesozoic a
594 Catalunya" (ref. CLT009/18/00066), based at the ICP and financially supported by the
595 Departament de Cultura (Generalitat de Catalunya). R.M.M. acknowledges the Linnean
596 Society of London for supporting this work throughout a Percy Sladen Memorial Fund
597 Grant. An anonymous reviewer and the editor (H.-D. Sues) provided helpful comments
598 and suggestions that greatly improved a previous version of the manuscript.

599

600 ## References

601

602 Beltan, L., 1972, La faune ichtyologique du Muschelkalk de la Catalogne: Memorias de
603 la Real Academia de las Ciencias y las Artes de Barcelona v. 41, p. 281–325.
604 Beltan, L., 1975, A propos de l'ichthyofaune triasique de la Catalogne espagnole:
605 Colloques Internationaux du Centre National de la Recherque Scientifique v. 218,
606 p. 273–280.
607 Brough, J., 1939, The Triassic fishes of Besano, Lombardy: British Museum (Natural
608 History), London, 177 p.
609 Bürgin, T., 1992, Basal ray-finned fishes (Osteichthyes; Actinopterygii) from the
610 Middle Triassic of Monte San Giorgio (Canton Tessin, Switzerland):
611 Schweizerische Paläontologische Abhandlungen v.114, p.1 – 164.
612 Calvet, F., and Tucker, M. E., 1988, Outer ramp cycles in the Upper Muschelkalk of the
613 Catalan Basin, northeast Spain: Sedimentary Geology v.57, p.185–198.
614 Calvet, F., and Marzo, M., ed., 1994, El Triásico de las Cordilleras Costero-Catalanas.
615 Estratigrafía, Sedimentología y Análisis Secuencial. Gráficas Cuenca, S.A.,
616 Cuenca, 53 p.
617 Calvet, F., March, M., and Pedrosa, A., 1987, Estratigrafía, sedimentología y diagénesis
618 del Muschelkalk superior de los Catalánides: Cuadernos de Geología Ibérica, v. 11,
619 p.171–198.
620 Calvet, F., Tucker, M.E., and Henton, J.M., 1990, Middle Triassic carbonate ramp
621 systems in the Catalan Basin, Northeast Spain: facies, systems tracts, sequences and
622 controls, *in* Tucker, M.E., Wilson, J. L., Crevello, P.D., Sarg, J.R., Read, J.F. eds.,

623 Carbonate Platforms: Facies, Sequences and Evolution: The International
624 Association of Sedimentologists v. 9, p. 79–108.
625 Calvet, F., Solé de Porta, N. and Salvany, J.M., 1993, Cronoestratigrafía (palinología)
626 del Triásico sudpirenaico y del Pirineo Vasco-Cantábrico: Acta Geologica
627 Hispanica v.28, p.33–48.
628 Calvet, F., Anglada, E. and Salvany, J.M., 2004, El Triásico de los Pirineos. *In* Vera
629 J.A. ed., Geología de España, Madrid, SGE-IGME, 272–274.
630 Calzada, S. and Magrans, J., 1997, Una nueva cita de *Lingula* en el Triásico pirenaico,
631 Batalleria, v. 7, p.45–46.
632 Cartanyà, J., 1999, An overview of the Middle Triassic actinopterygians from Alcover,
633 Mont-ral and El Pinetell (Catalonia, Spain). *In* Arratia G. and Schultze H.P., eds,
634 Mesozoic fishes 2 - Systematics and the fossil record, Pfeil verlag, p. 535– 551.
635 Cartanyà, J., Fortuny, J., Sellés, A.G., Bolet, A., Petruzzelli, M., Solà, E., Sagarra. and
636 Galobart, A., 2011, Preliminary report on the vertebrate assemblage of the Odèn
637 outcrops (Carnian, Late Triassic) of the Pyrenean Basin, Catalonia. *In* Marigó, J.,
638 Pérez de los Ríos, M., Minwer-Barakat, R., Bolet, A. and De Miguel, D., eds.,
639 XXVII Jornadas de la Sociedad Española de Paleontología y Simposios de los
640 Proyectos PICG 587 y 596: Sabadell, Paleontologia i Evolució, Memòria Especial,
641 v5, p.59–61.
642 Cartanyà, J**.,** Fortuny, J., Bolet, A., Mutter, R., 2015, *Colobodus giganteus* (Beltan,
643 1972) comb. nov. from the Upper Muschelkalk Facies of Catalonia (NE Iberian
644 Peninsula): Neues Jahrbuch für Geologie und Paläontologie, Abhandlungen, v.278,
645 p. 323–333.
646 Cartanyà, J., Fortuny, J., Bolet, A. and Garcia-Artigas, R., 2019, *Moradebrichthys*
647 *vilasecae* gen. et sp. nov., a new perleidid (Actinopterygii: Osteichthyes) from the

Middle Triassic of Catalonia (NE Iberian Peninsula): Neues Jahrbuch für Geologie und Paläontologie, Abhandlungen v. 292, p.171–190.

Cope, E.D., 1887, General notes: geology and palaeontology. IV: American Naturalist, v. 21, p.1016–1019.

Escudero-Mozo, M.J., Márquez-Aliaga, A., Goy, A., Martín-Chivelet, J., López-Gómez, J., Márquez, L., Arche, A., Plasencia, P., Pla, C., Marzo, M., and Sánchez-Fernández, D., 2015, Middle Triassic carbonate platforms in eastern Iberia: Evolution of their fauna and palaeogeographic significance in the western Tethys: Palaeogeography, Palaeoclimatology, Palaeoecology v. 417, p. 236–260.

Fréchengues, M., and Peybernès, B., 1991a. Associations de Foraminifers benthiques dans le Trias carbonaté (Anisien, Ladinien-Carnien et Rhéthien) des Pyrénées Espagnoles: Acta Geologica Hispánica, v.26, p.67–73.

Fréchengues, M., and Peybernès, B., 1991b. Stratigraphie séquentielle du Trias moyen et supérieur des Pyrénées franco espagnoles: Comptes Rendus de l'Académie des Sciences, Paris, v.313, p.355–360.

Fréchengues, M., Martim, R., Peybernes, B., and Zaninetti, L., 1990., Mise en évidence d' associations de Foraminiferes benthiques dans la séquence de déposit Ladino-Carnienne du "Muschelkalk" des Pyrénées Catalanes (France, Espagne). Comptes Rendus de l'Académie des Sciences, Paris, v.310, p.667–673.

Fréchengues, M., Peybernes, B., Thiébaut, J., Durand-Wackenheim, C., Fournier-Vinas, C., and Lucas, C., 1991, Mise en évidence d' un volcanisme acide de type explosif dans le "Muschelkalk" des Pyrénées franco-espagnoles (Séquence de dépôt Sd 237, Anisien supérieur-Ladinian inférieur) : Bulletin de la Société d'Histoire Naturelle de Toulouse, v.127, p. 111–118.

672 Fréchengues, M., Peybenes, B., Lucas, C., and Souquet, P., 1992, Le Trias des Pyrénées
673 centrales et orientales Franco- Espagnoles, Livret-Guide: Strata, v.17, p.1–90.
674 Fortuny, J., Bolet, A., Sellés, A.G., Cartanyà, J., and Galobart, A., 2011, New insights
675 on the Permian and Triassic vertebrates from the Iberian Peninsula with emphasis
676 on the Pyrenean and Catalonian basins: Journal of Iberian Geology, v.37, p.65–86.
677 Furrer, H., Schaltegger, U., Ovtcharova, M., and Meister, P., 2008, U-Pb zircon age of
678 volcaniclastic layers in Middle Triassic platform carbonates of the Austroalpine
679 Silvretta nappe (Switzerland): Swiss Journal of Geosciences, v.101, p. 595–603.
680 García-Ávila, M., Mercedes-Martín, R., Juncal M.A., Diez, J.B., 2020, New
681 palynological data in Muschelkalk facies of the Catalan CoastalRanges (NE of the
682 Iberian Peninsula): Comptes Rendus Géoscience, v.352, p.443–454.
683 Gardiner, B.G., 1967, Further notes on palaeoniscoid fishes with a classification of the
684 chondrostei: Bulletin of the British Museum (Natural History), Geology, v.14,
685 p.143 – 206.
686 Hemleben, C., and Freels, D., 1977, Fossilführende dolomitisierte Plattenkalke aus dem
687 “Muschelkalk superior” bei Montral (Prov. Tarragona, Spanien): Neues Jahrbuch
688 für Geologie und Paläontologie, Abhandlungen, v.154, p.186–212.
689 Kner, R., 1866, Die Fische der bituminösen Schiefer von Raibl in Kärnthen:
690 Sitzungsberichte der Akademie der Wissenschaften in Wien, v.53, p.152–197.
691 Lehman, J.P., 1964, Étude d’un saurichthyidé de la región d’Odèn (Espagne): Annales
692 de Paleontologie (Vertébrés), v.50, p.23–30.
693 Lombardo, C., 1999. Sexual dimorphism in a new species of the actinopterygian
694 *Peltopleurus* from the Triassic of Northern Italy: Palaeontology, v.42, p.741 – 760.
695 López-Gómez, J., Alonso-Azcárate, J., Arche, A., Arribas, J., Barrenechea, J. F.,
696 Borruel-Abadía, V., and Díez, J.B., 2019, Permian-Triassic Rifting Stage. *In*

Quesada, C., Oliveira, J.T., eds. The Geology of Iberia: A Geodynamic Approach Springer, Berlin, p. 29–112.

Mercedes-Martín, R., and Buatois, L., 2021, Microbialites and trace fossils from a Middle Triassic restricted carbonate ramp in the Catalan Basin (Spain): evaluating environmental and evolutionary controls in an epicontinental setting: Lethaia. https://doi.org/10.1111/let.12378.

Mercedes-Martín, R., Arenas, C., and Salas, R., 2014, Diversity and factors controlling widespread occurrence of syn-rift Ladinian microbialites in the western Tethys (Triassic Catalan Basin, NE Spain): Sedimentary Geology, v.313, p. 68–90.

Ramos, A., Sopeña, A., Sánchez-Moya, A., and Muñoz, A., 1996. Subsidence analysis, maturity modelling and hydrocarbon generation of the Alpine sedimentary sequence in the NW of the Iberian Ranges (Central Spain): Cuadernos de Geología Ibérica, v.21, p. 23–53.

Salas, R., and Casas, A., 1993, Mesozoic extensional tecton- ics, stratigraphy and cristalevolution turing the Alpine cycle of the eastern Iberian basin: Tectonophysics, v.228, p.33–55.

Salas, R., Guimera, J., Mas, R., Martin-Closas, C., Melendez, A., and Alonso, A., 2001. Evolution of the mesozoiccen-traliberian Rift System and its Cainozoic inversion (Iberian chain), *in* Ziegler, P.A., Cavazza, W., Robertson, A.H.F., Crasquin-Soleau, S., eds., Peri-Tethys Memoir 6: Peri-Tethyan Rift/Wrechn Basins and Passive Margins: Mémoires du Museum national d'Histoire naturelle, v.186, p.145–185.

Salvany, J. M., Ortí, F., 1987. El Keuper de los Catalánides: Cuadernos de Geología Ibérica, v.11, p. 215–236.

Schmidt, M., 1935, Fossilien der Spanischen Trias: Abhandlungen der Heidelberger Akademie der Wissenschaften v.22, p.1–140.

722 Tintori, A., 1990, The actinopterygian fish *Prohalecites* from the Triassic of northern
723 Italy: Palaeontology, v.33, 155–174.
724 Verneuil, E., 1854, Descubrimiento de *Ceratites* en Mora de Ebro: Revista Minera v.5,
725 p.676–677.
726 Via-Boada, L., Villalta, J. F., Esteban-Cerdá, M., 1977, Paleontología y paleoecología
727 de los yacimientos fosilíferos del Muschelkalk superior entre Alcover y Mont-ral
728 (Montañas de Prades, Provincia de Tarragona): Cuadernos de Geología Ibérica, v.
729 4, p. 247–256.
730 Virgili, C., 1958, El Triásico de los Catalánides: Boletín del Instituto Geológico y
731 Minero v.69, p.1– 856.
732 Virgili, C., Sopena, A., Arche, A., Ramos, A., and Hernando, S., 1983, Some
733 observations on the Triassic of the Iberian Peninsula: Neue Beiträge zur
734 Biostratigraphie der Tethys-Trias, Schriftenreihe der Erdwissenschaftalichen
735 Kommission, v.5, p.287–294.
736 Wu, F.X., Sun, Y.L., Xu, G.H., Hao, W.C., Jiang, D.Y., and Sun, Z.Y., 2011, New
737 saurichthyid actinopterygian fishes from the Anisian (Middle Triassic) of
738 southwestern China: Acta Palaeontologica Polonica v.56, p. 581–614.
739 Wurm, A., 1913, Beiträge zur Kenntnis der iberisch-balearisehen Trias Provinz:
740 Verhandlungen des Naturhistorich-medizinischen Vereins zu Heidelberg v.12,
741 p.477–594.
742 Xu, G. H., and Ma, X. Y., 2016, A Middle Triassic stem-neopterygian fish from
743 China sheds new light on the peltopleuriform phylogeny and internal
744 fertilization. Chinese Science Bulletin v.61, p.1766–1774.
745 Xu, G. H., Ma, X. Y., and Zhao, L. J., 2018, A large peltopleurid fish (Actinopterygii:
746 Peltopleuriformes) from the Middle Triassic of Yunnan and Guizhou, China.

747 Vertebrata PalAsiatica v.56, p.106–120.

748

749 **Figures**

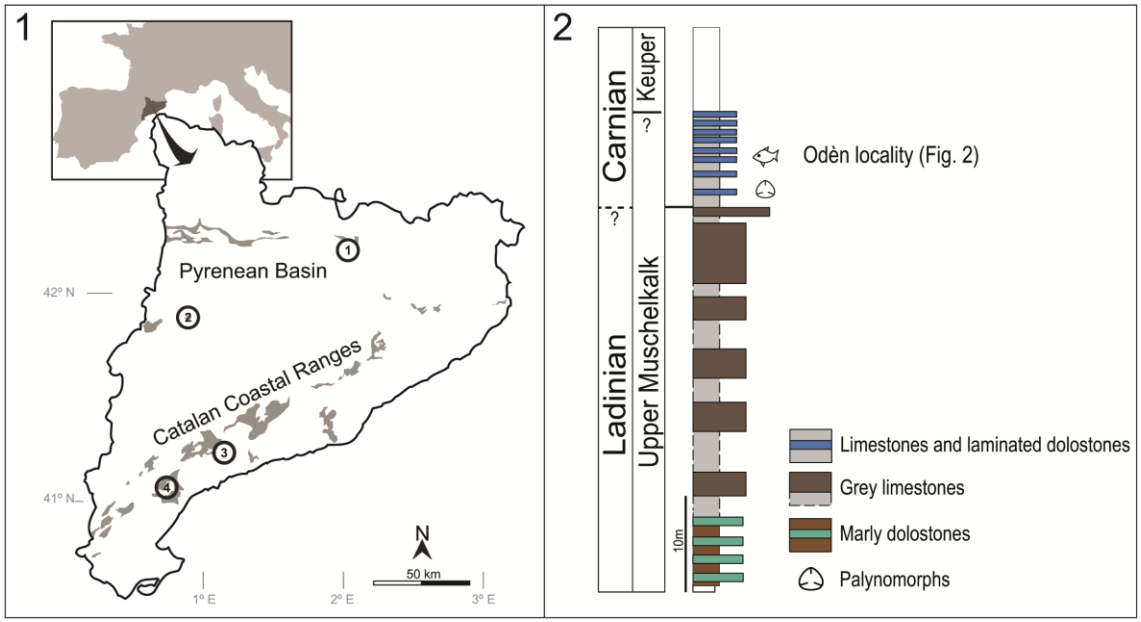

750

751 **Figure 1**. (1) Location of the Middle Triassic Pyrenean basin in Catalonia (NE Iberian

752 Peninsula, Spain) with the localities mentioned in the text: 1) Odèn. 2) Vilanova de la

753 Sal. 3) Mont-ral - Alcover. 4) Mora d'Ebre - Camposines. (2) Synthetic stratigraphic

754 section for Odèn locality (modified from Calvet et al., 1993).

755

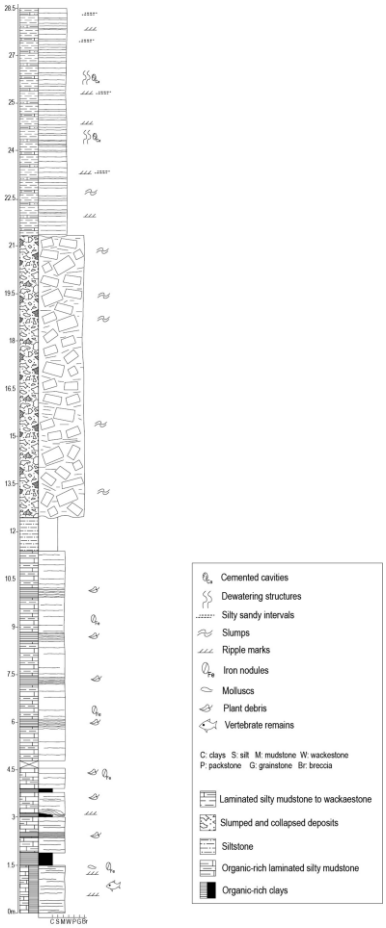

Figure 2. Sedimentary log in Odèn outcrop. Fossil-bearing units are referred to the bottom units.

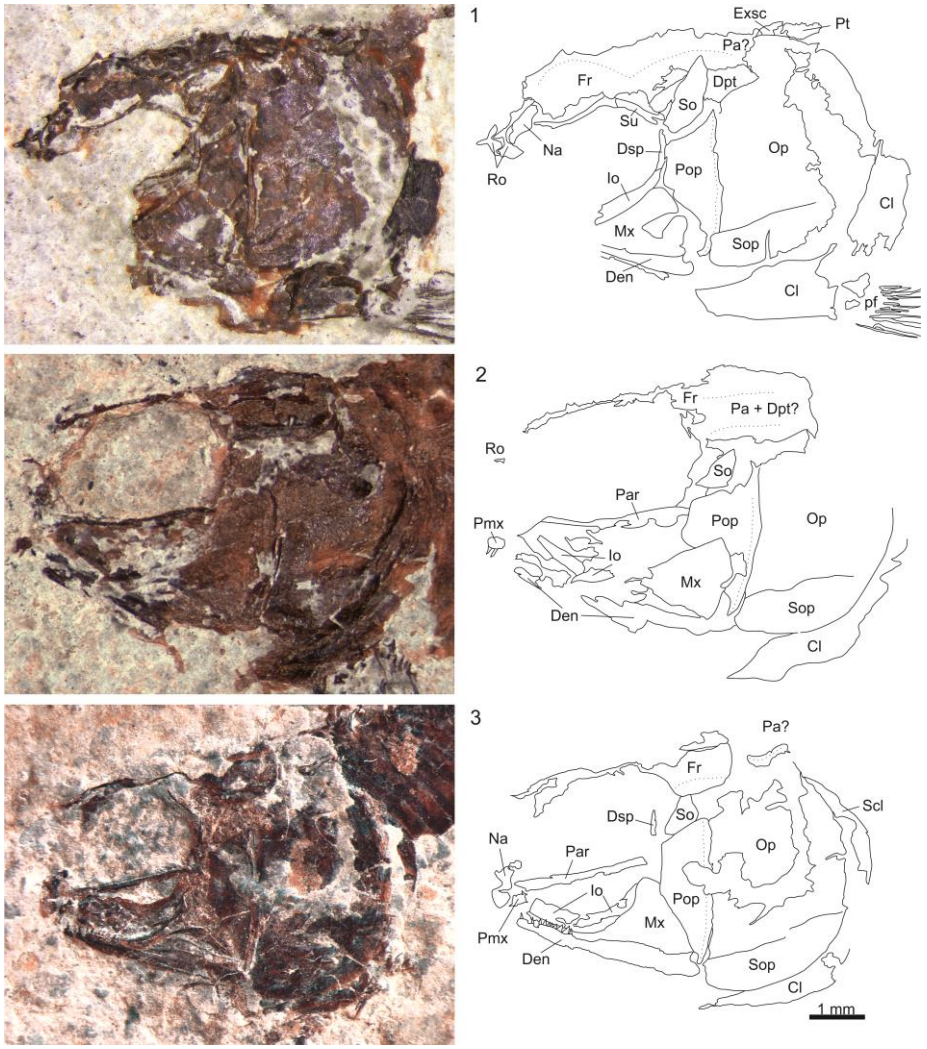

760

761 **Figure 3**. *Peltopleurus* cf. *P. nuptialis.* Nearly complete skulls with a drawing of the

762 identified bones, the doted lines represent sensory canals. (1) IPS106977. (2)

763 IPS122561. (3) IPS107023. Cl, cleithrum; Den, dentary bone; Dpt, dermopterotic; Dsp,

764 dermosphenotic; Exsc, extrascapular; Fr, frontal; Io, infraorbital; Mx, maxilla; Na,

765 nasal; Op, operculum; Pa, parietal; Par, Parasphenoid; pf, pectoral fin; Pmx, premaxilla;

766 Pop, preoperculum; Pt, posttemporal; Ro, rostral; Scl, supracleithrum; So, suborbital;

767 Sop, suboperculum; Su, supraorbital.

768

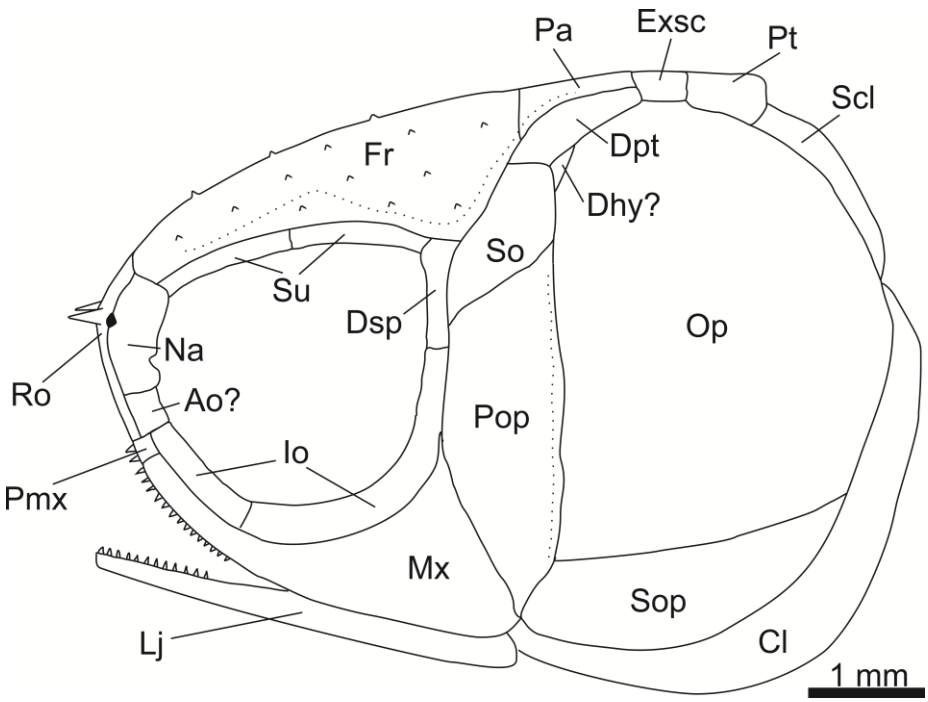

769

770 **Figure 4**. *Peltopleurus* cf. *P. nuptialis.* Idealized reconstruction of the skull based on

771 the combined observations of the specimens studied. Ao, antorbital; Cl, cleithrum; Dhy,

772 dermohyal; Dpt, dermopterotic; Dsp, dermosphenotic; Exsc, extrascapular; Fr, frontal;

773 Io, infraorbital; Lj, lower jaw; Mx, maxilla; Na, nasal; Op, operculum; Pa, parietal;

774 Pmx, premaxilla; Pop, preoperculum; Pt, posttemporal; Ro, rostral; Scl, supracleithrum;

775 So, suborbital; Sop, suboperculum; Su, supraorbital.

776

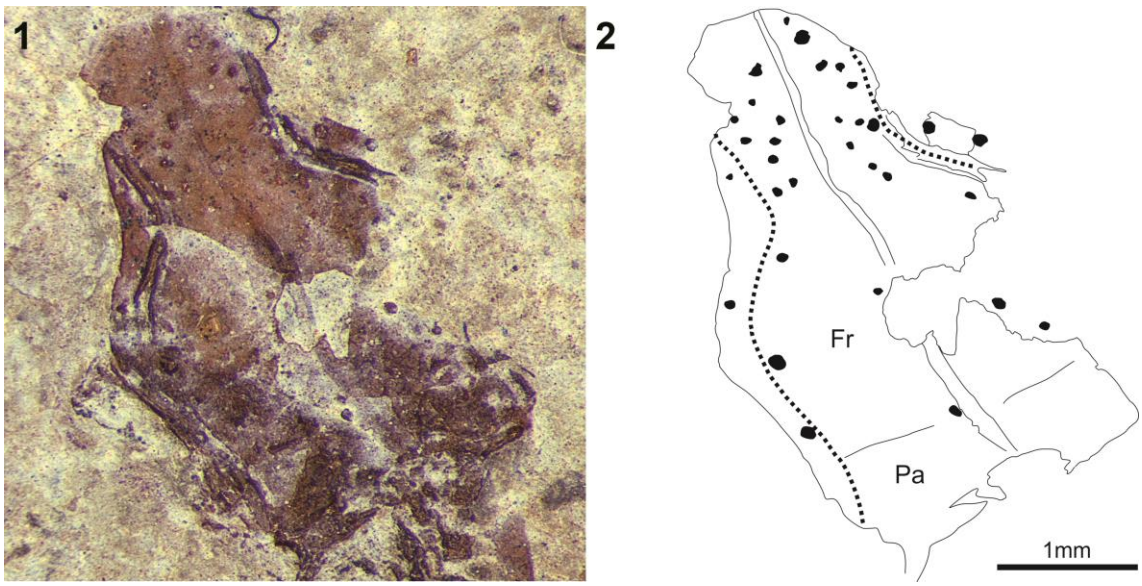

777

Figure 5. *Peltopleurus* cf. *P. nuptialis.* Skull roof of the specimen IPS85811 showing the small conical tubercles randomly arranged on the frontal bone (black dots) and the supraorbital sensory canal (dotted lines). (1) Photograph. (2) Interpretative drawing. Fr, frontal; Pa, parietal.

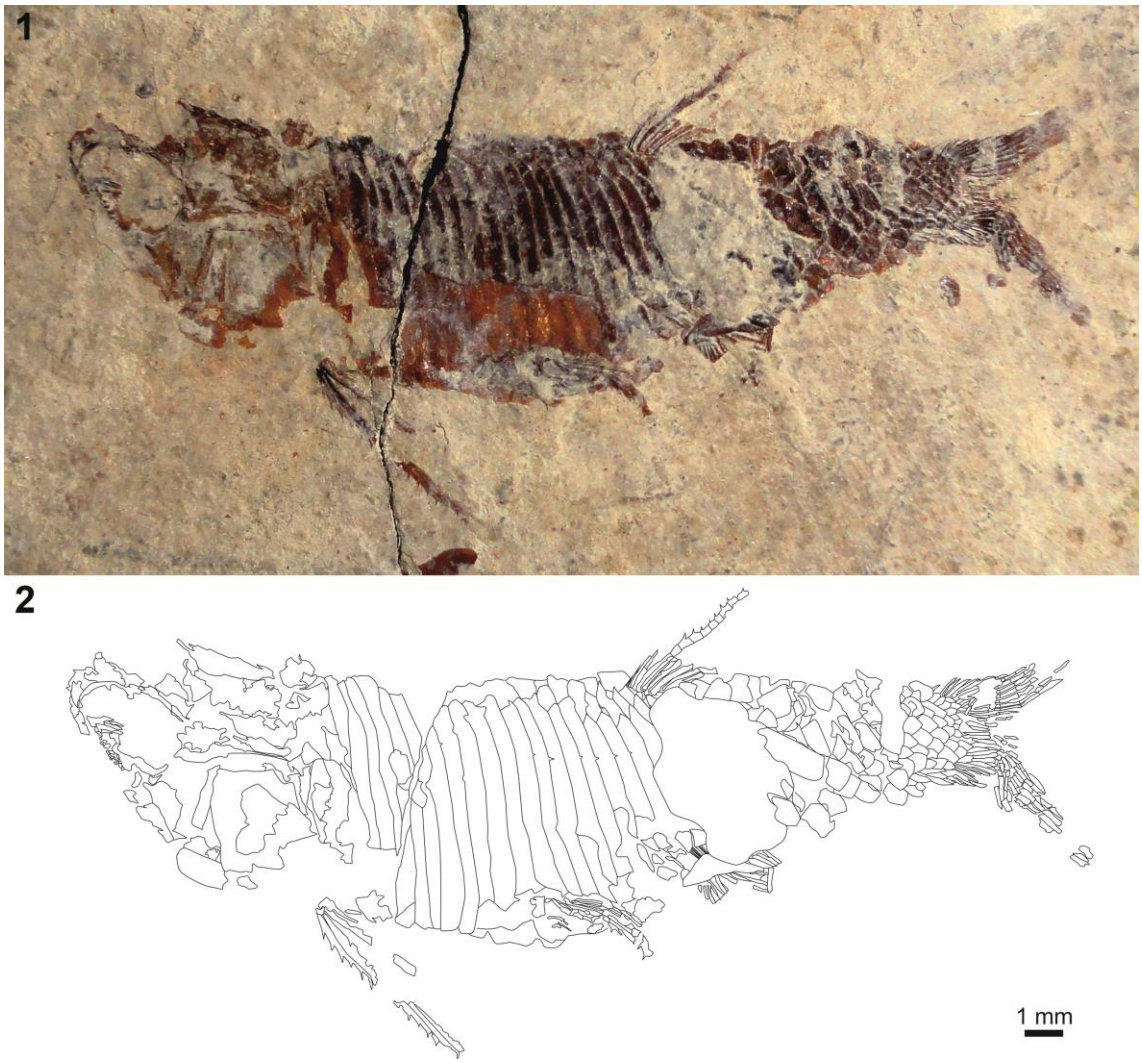

Figure 6. *Peltopleurus* cf. *P. nuptialis.* IPS86048, a nearly complete body with its skull disarticulated. (1) Photograph. (2) Interpretative drawing. In this morphotype B specimen it is possible to identify the long dorsal and pectoral fins with their hooks, the pelvic fins with its hooks, the anal fin partially covered by the scute and the caudal fin.

788

789 **Figure 7**. *Peltopleurus* cf. *P. nuptialis.* (1) IPS86048 and (2) IPS85919., detail of the

790 long pectoral and dorsal fins with their hook structure on the anterior margin of the

791 segments. (3) IPS106909, detail of the skull showing the lines of flattened oval teeth.

792

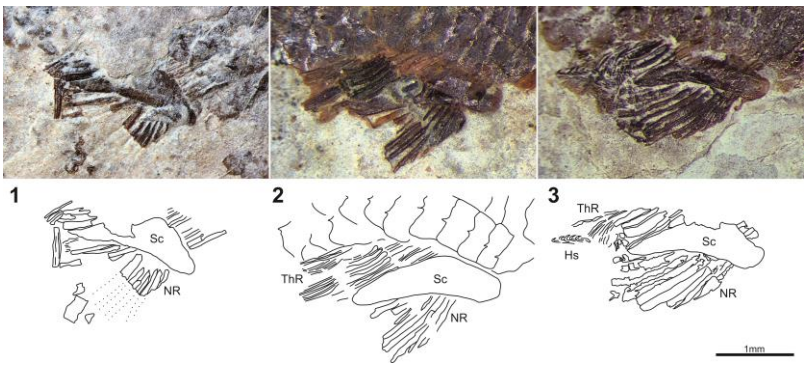

793

794 **Figure 8**. *Peltopleurus* cf. *P. nuptialis.* Morphotype B anal fins showing the described

795 structure composed by normal rays (NR) bearing hooks on each segment, a series of

796 thin rays (ThR) ending in small sharp hooks (Hs) and a triangular scute (Sc) covering

797 the fin. (1) IPS86048. (2) IPS106957. (3) IPS106902.

798

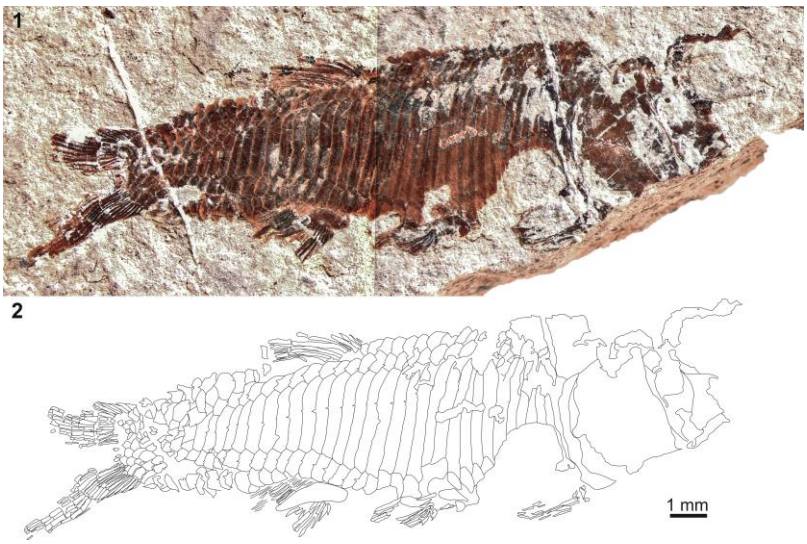

799

Figure 9. *Peltopleurus* cf. *P. nuptialis.* IPS106957, a nearly complete body missing the anterior portion. This morphotype B specimen shows the main features of the squamation. (1) Photograph. (2) Interpretative drawing.

Figure 10. Additional faunas recovered from the studied section. (1) *Pseudocorbula gregaria* (IPS123389). (2) Sauropterygian rib (IPS-86018). (3) small robust dentary from an unidentified actinopterygian (IPS122539).

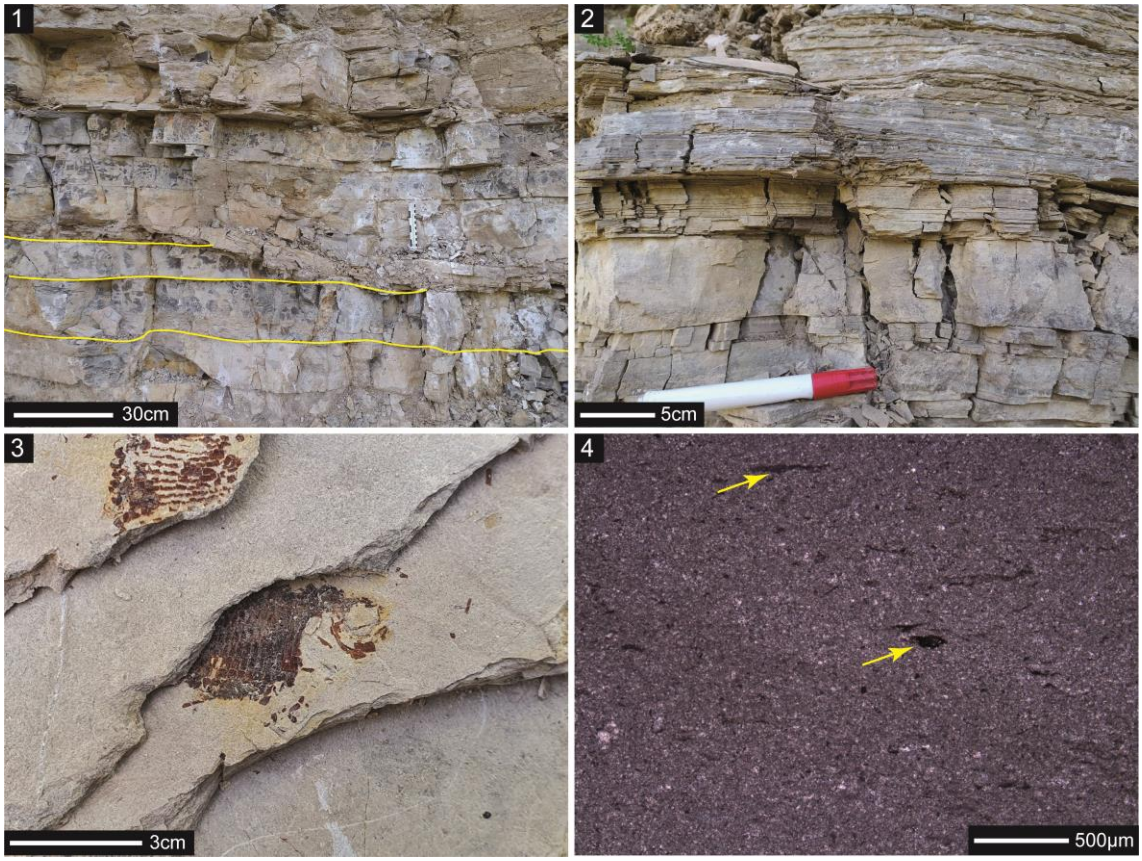

Figure 11. Organic-rich laminated silty mudstone (Facies association 1). (1) Massive tabular beds showing channel-fill with cross-bedded bundles over erosional surfaces. (2) Massive beds alternate with finely laminated, fossil-bearing mudstones (top). (3) Actinopterygian remains in the top laminae of the finely laminated facies. (4) Photomicrograph of organic-rich micritic mudstone with floral remains (arrows).

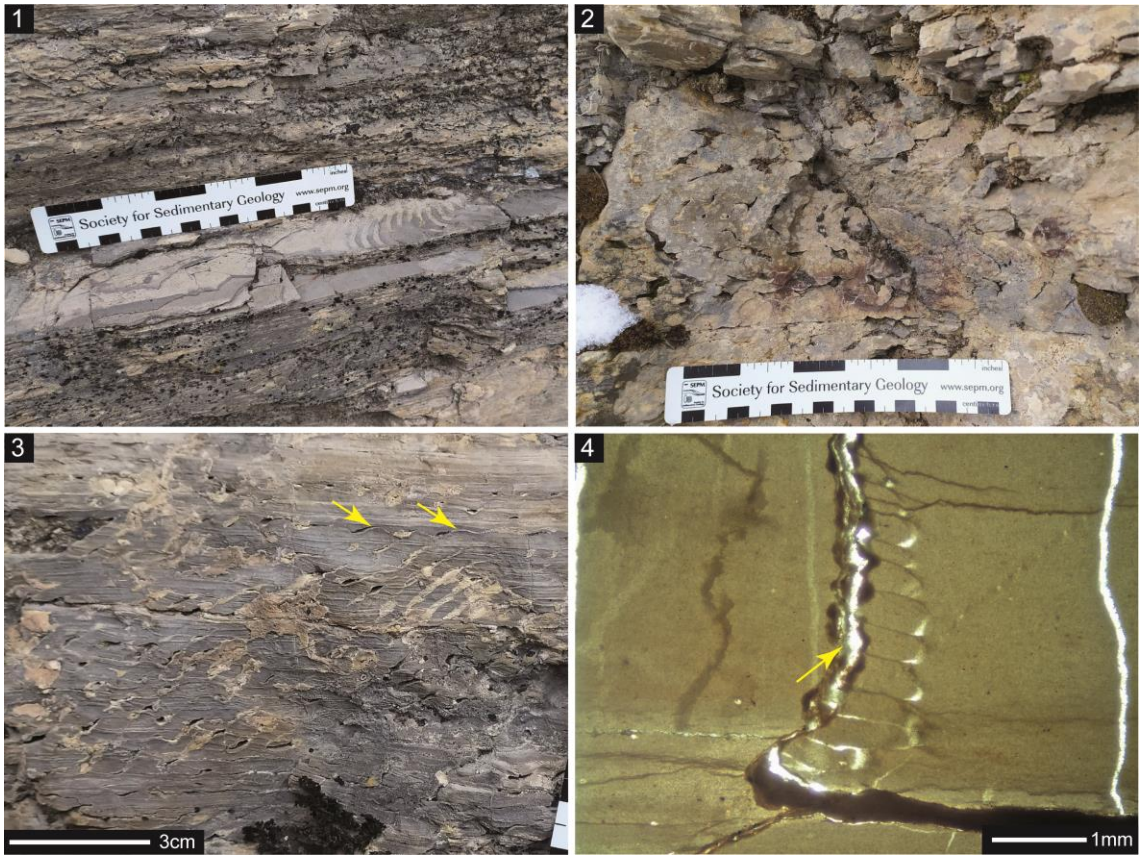

Figure 12. Laminated silty mudstone to wackestone (Facies association 2). (1) Laminated mudstone to wackestone units showing wave ripple structures with straight, symmetrical, and parallel crests. Note silt-rich intervals in pale brown color. (2) Dewatering structures tend to form open conduits producing vertically folded structures. (3) Waterscape conduits can be at 45º to 80º from ripple planes (arrows) which are partially filled by silt or cement. (4) Photomicrograph of dewatering flame structures filled by calcite cement.

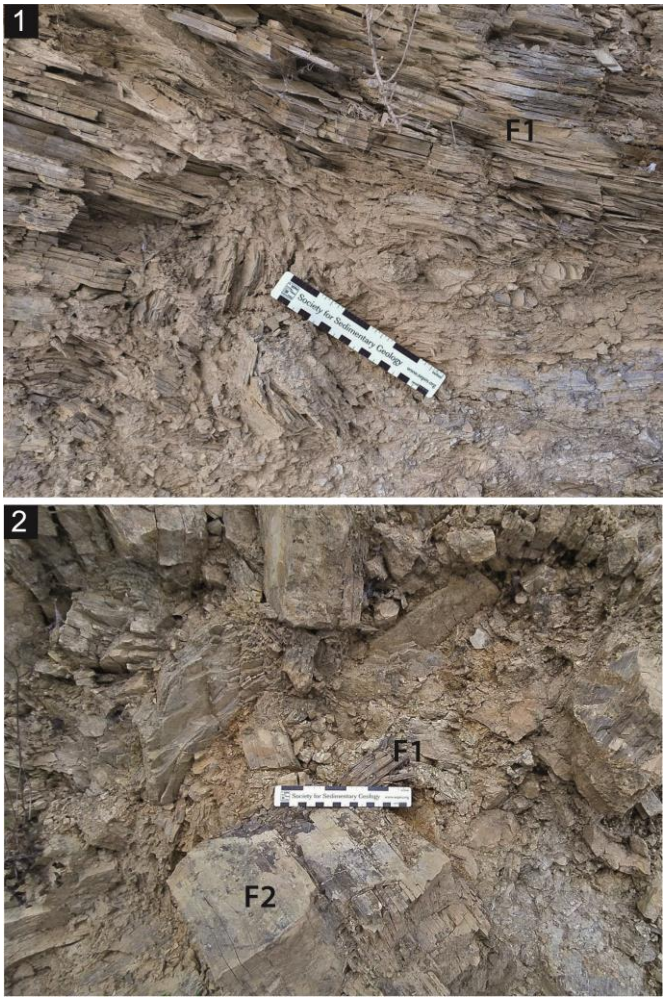

826

827 **Figure 13**. Slumped and contorted breccia deposits (Facies association 3). (1) Detail of
828 slumped organic-rich laminated facies (Facies association 1, F1), (2) In some settings,
829 slumped and collapsed beds are dominated by poorly sorted, mostly clast-supported
830 breccia and blocks of Facies association 2 (F2).

831

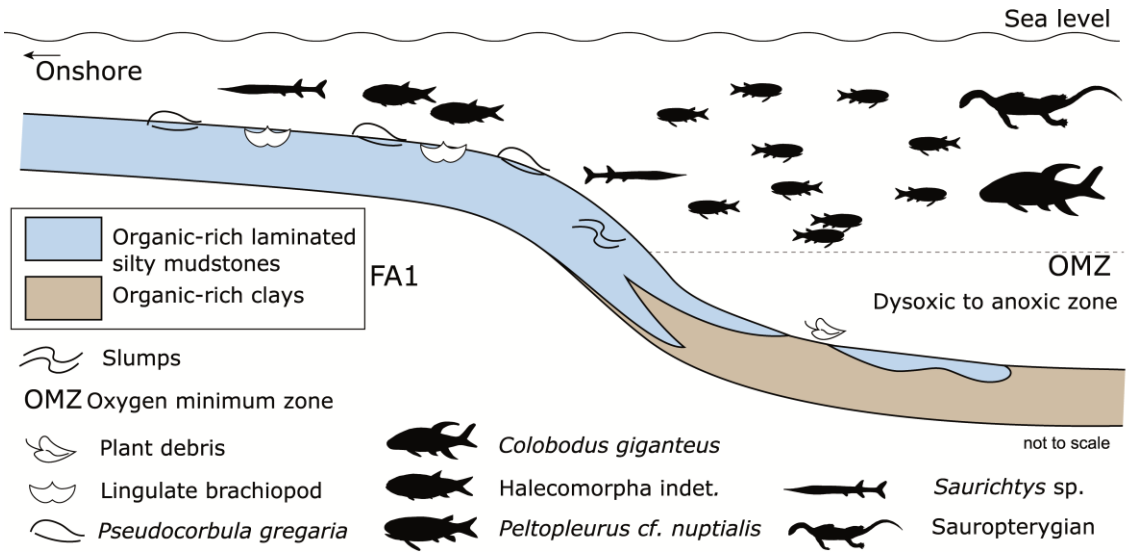

832

833 **Figure 14.** Schematic paleoenvironmental reconstruction of Facies Association 1 (FA1)

834 which contains the macrofauna studied in this work.